Aerosol Science and Technology
Publication details, including instructions for authors and subscription information:
http://www.tandfonline.com/loi/uast20

A Methodology for Measuring Size-Dependent Chemical Composition of Ultrafine Particles

Michael D. Geller , Seongheon Kim , Chandan Misra , Constantinos Sioutas , Bernard A. Olson & Virgil A. Marple
Published online: 30 Nov 2010.

To cite this article: Michael D. Geller , Seongheon Kim , Chandan Misra , Constantinos Sioutas , Bernard A. Olson & Virgil A. Marple (2002) A Methodology for Measuring Size-Dependent Chemical Composition of Ultrafine Particles, Aerosol Science and Technology, 36:6, 748-762, DOI: 10.1080/02786820290038447

To link to this article: http://dx.doi.org/10.1080/02786820290038447

Aerosol Science and Technology 36: 748–762 (2002)

Published by Taylor and Francis
0278-6826/02/$12.00 + .00
DOI: 10.1080/0278682029003844 7

A Methodology for Measuring Size-Dependent Chemical Composition of Ultrafine Particles

Michael D. Geller,[1] Seongheon Kim,[1] Chandan Misra,[1] Constantinos Sioutas,[1] Bernard A. Olson,[2] and Virgil A. Marple[2]

[1] *Civil and Environmental Engineering, University of Southern California, Los Angeles, California*
[2] *Mechanical Engineering, University of Minnesota, Minneapolis, Minnesota*

Ultrafine particulate matter (PM) consists of particles mostly emitted by combustion sources but also formed during gas-to-particle formation processes in the atmosphere. Various studies have shown these particles to be toxic. The very small mass of these particles has posed a great challenge in determining their size-dependent chemical composition using conventional aerosol sampling technologies. Implementing 2 technologies in series has made it possible to overcome these 2 problems. The first technology is the USC Ultrafine Concentrator, which concentrates ultrafine particles (i.e., 10–180 nm) by a factor of 20–22. Ultrafine particles are subsequently size fractionated and collected on suitable substrates using the NanoMOUDI, a recently developed cascade impactor that classifies particles in 5 size ranges from 10 to 180 nm.

The entire system (concentrator + NanoMOUDI) was employed in the field at 2 different locations in the Los Angeles Basin in order to collect ultrafine particles in 3 consecutive 3 h time intervals (i.e., morning, midday, and afternoon). The results indicate a distinct mode in the 32–56 nm size range that is most pronounced in the morning and decreases throughout the day at Downey, CA (a "source" site), affected primarily by vehicular PM emissions. While the mass concentrations at the source site decrease with time, the levels measured at Riverside, CA (a "receptor" site), are highest in the afternoon with a minimum at midday. In Riverside, ultrafine EC (elemental carbon) and OC (organic carbon) concentrations were highly correlated only during the morning period, whereas these correlations collapsed later in the day. These results indicate that in this area, ultrafine PM is generated by primary emissions during the morning hours, whereas secondary aerosol formation processes become more important as the day progresses.

Received 9 July 2001; accepted 31 October 2001.

This work was supported in part by the Southern California Particle Center and Supersite (SCPCS), funded by the U.S. EPA under the STAR program, and the California Air Resources Board. Although the research described in this article has been funded in part by the United States Environmental Protection Agency through grants 53-4507-0482, 53-4507-7721, and 53-4507-8360 to USC, it has not been subjected to the Agency's required peer and policy review and therefore does not necessarily reflect the views of the Agency and no official endorsement should be inferred.

Address correspondence to Michael D. Geller, University of Southern California, Department of Civil and Environmental Engineering, 3620 South Vermont Avenue, Los Angeles, CA 90089. E-mail: mgeller@usc.edu

INTRODUCTION

Increased concentrations of airborne particulate matter (PM) have been positively correlated with mortality and morbidity rates (Dockery et al. 1993; Pope et al. 1995). Although epidemiological studies to date have not made it perfectly clear whether it is particle mass, surface area, or number concentrations that may be responsible for these observed health outcomes presumably attributable to PM, certain toxicological investigations suggest that atmospheric ultrafine particles may be responsible for some of these adverse effects (Oberdoerster et al. 1992, 1995; Donaldson and MacNee 1998).

Atmospheric ultrafine particles, defined as particles with diameters $<0.1\ \mu$m, exist at concentrations of approximately 10,000–30,000 particles per cm^3 of air within cities and arise from either gas-to-particle conversion processes—in which hot, supersaturated vapors undergo condensation upon being cooled to ambient temperatures—and/or are directly emitted as products of incomplete combustion processes (Whitby and Svendrup 1980). While these particles dominate the atmospheric particle number concentrations, they amount to a negligible contribution of atmospheric particle mass concentrations. A given mass of ultrafine particles, however, has 100–1000 times more surface area than an equal mass of fine particles ($0.1\ \mu$m < diameter < $2.5\ \mu$m) and approximately 10^5 times more surface area than an equal mass of coarse particles ($2.5\ \mu$m < diameter < $10\ \mu$m) (Harrison et al. 2000), which may significantly affect their relative toxicity. Because of their increased number and surface area, ultrafine particles are particularly important in atmospheric chemistry and environmental health.

To date there has been limited, but rapidly increasing, toxicological and epidemiologicalevidence linking respiratory

health effects and exposure to ultrafine particles. The limited data are primarily due to lack of adequate methods for ultrafine particle sampling and measurement. Since little is known about the chemical composition of ultrafine PM, no one has yet determined whether particle numbers or chemical constituents make this mode a human health risk. Limited studies on the 24 h averaged chemical composition of ambient ultrafine particles in cities have been recorded prior to the work presented in this paper (Hughes et al. 1998; Cass et al. 2000), and no previous research has been conducted on size-segregated ultrafine particle mass concentrations below 56 nm. Since the values of atmospheric parameters influencing ambient ultrafine particle concentration and chemical composition, such as the emission strengths of particle sources, temperature, relative humidity (RH), wind direction and speed, and mixing height, fluctuate in time scales that are substantially shorter than 24 h, 24 h measurement may not be particularly revealing on the formation mechanisms of these particles. Shorter time-scale data on the physico-chemical characteristics of ultrafine particles are thus essential in order to understand their atmospheric properties, human exposure, and ultimately their health effects.

The work presented in this paper is intended to introduce a technology that will add to the body of knowledge surrounding the chemical composition and mass concentrations of specific size ranges of ultrafine particles. Two locations in southern California—Downey and Riverside—served as sampling locations in order to compare the ultrafine mass concentrations and chemical compositions over different time periods during which ultrafine PM size distribution and chemical composition are affected by different sources and formation mechanisms.

METHODS

Sampler Description

The collection of size-fractionated ultrafine particles was accomplished by using 2 technologies in tandem. A USC Ultrafine Concentrator was connected upstream of a nano-micro-orifice uniform deposited impactor (Nano-MOUDI, MSP Corporation, Minneapolis, MN). Figure 1 illustrates the USC Ultrafine Concentrator/Nano-MOUDI complex.

The USC Ultrafine Concentrator is capable of enriching the concentration of particles by a factor of up to 40, depending on the output flow rate (Sioutas et al. 1999; Kim et al. 2000a,b, 2001a,b). Concentration enrichment of ultrafine particles is accomplished by first drawing air samples at a sampling flow of 220 l min^{-1} through a saturation-condensation system that grows particles to 2–3 μm droplets, which are subsequently concentrated by virtual impaction and are finally returned to their original size distributions after passing through diffusion dryers. The USC Ultrafine Concentrator used in this study consists of 2 parallel sampling lines, each operating at an intake flow rate and an output flow rate of 110 l min^{-1} and 5 l min^{-1}, respectively, therefore achieving an ideal concentration enrichment by twenty-two-fold.

After the ultrafine particles were concentrated, they were drawn first through a MOUDI and then through a Nano-MOUDI. The full MOUDI was needed upstream of the Nano-MOUDI in order to create the correct pressures necessary in the Nano-MOUDI stages for impaction of ultrafine particles. The higher stages of the MOUDI were also used to remove particles larger than 180 nm from the air sample, which were of no interest to this study. Although the definition of ultrafine particles typically involves particles smaller than 100 nm, particles in the size range of 100 to 180 nm were also sampled and analyzed chemically because they represent a transition zone from the ultrafine to the accumulation mode.

The Nano-MOUDI is a cascade impactor operating under a very low pressure that attaches to the MOUDI after the 56 nm cut-point stage and includes 3 stages with cut points of 32 nm, 18 nm, and 10 nm, respectively (Marple and Olson 1999). An Electrical Low Pressure Impactor (ELPI) pump (Model 393501, TSI, Inc., St. Paul, MN) was used to draw 10 l min^{-1} under the necessary vacuum. The Nano-MOUDI operates based on the Stoke's impaction formula with emphasis given to the

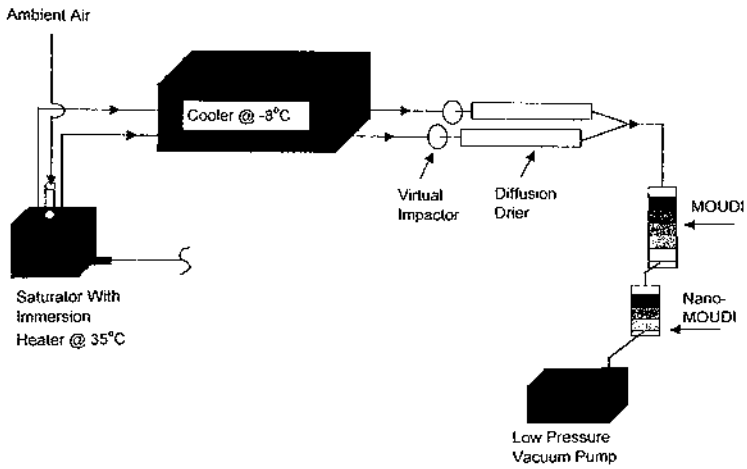

Figure 1. Schematic diagram of the tandem USC Ultrafine Particle Concentrator and the Nano-MOUDI.

Table 1
MOUDI and nano-MOUDI design parameters

Stage	Nominal cut point μm	Calibrated[a] cut point μm	Nozzle diameter cm	No. of nozzles	S/W[b]	P/P_o[c]	Nozzle Reynolds number[d]
8	0.18	0.18	0.0090	900	6.4	0.89	580
9	0.10	0.097	0.0055	2000	10.6	0.76	500
10	0.056	0.057	0.0052	2000	11.1	0.59	750
11	0.032	0.032	0.0049	980	11.9	0.40	290
12	0.018	0.018	0.0045	1650	13.0	0.23	200
13	0.010	—	0.0050	2000	11.4	0.12	160

[a]Based on a flow rate of 30 l min^{-1} for MOUDI stages 8–10 and 10 l min^{-1} for Nano-MOUDI stages 11–13 at standard atmospheric temperature and pressure.
[b]S = jet-to-plate distance; W = nozzle diameter.
[c]P = absolute pressure at stage exit with all upstream stages present; P_o = pressure at MOUDI inlet.
[d]Reynolds number (Re) is defined as Re = $U D/v$, where U and D are the jet velocity and diameter of a given stage, respectively, and v is the dynamic air viscosity.
Source: Marple and Olson (1999).

Cunningham slip correction factor, C_c.

$$\mathrm{St} = \frac{\rho_p U_i d_p^2 C_c}{9\mu d_o}, \qquad [1]$$

where d_p, ρ_p, and C_c are the particle diameter, density, and slip correction, μ is the air viscosity (1.81×10^{-4} g/cm·s), U_i is the velocity through the acceleration nozzle, and d_o is the inside diameter of the nozzle. Table 1 lists the various stages with their cut points and other pertinent information.

The Nano-MOUDI has a design flow rate of 10 l min^{-1}, while the MOUDI is designed for 30 l min^{-1}. In order to match the flow of the MOUDI to that of the Nano-MOUDI without changing the cutpoints of the MOUDI stages, the acceleration nozzle plates of the regular MOUDI were carefully masked so that two-thirds of the acceleration nozzles were blocked. A flow of 10 l min^{-1} could then be pulled through the MOUDI, instead of its design flow rate of 30 l min^{-1}, while maintaining the original cut points of each stage.

Laboratory Characterization of the USC Ultrafine Concentrator

The USC Ultrafine Concentrator was first characterized in the laboratory in order to evaluate its ability to concentrate ultrafine particles in the range of 10 to 180 nm without any dependence of the concentration enrichment on particle size or chemical composition. The system was operated under normal conditions for 3 test aerosol types—indoor air, laboratory-generated polydisperse ammonium sulfate, and laboratory-generated polydisperse ammonium nitrate aerosols. These aerosols were tested in order to ensure that the concentrator's efficiency was not affected by chemical composition of the aerosol. Polydisperse aerosols were generated by atomizing dilute aqueous solutions of ammonium sulfate and ammonium nitrate particles with a constant output nebulizer (HOPE, B & B Medical Technologies, Inc., Orangevale, CA) at a rate of 15 l min^{-1}. The generated particles were drawn through a 2 l glass container in which they were mixed with dry room air in order to remove excess moisture. The dry aerosols were then drawn through a series of Po-210 neutralizers (NDR Inc., Grand Island, NY) that reduced particle charges before entering the USC Ultrafine Concentrator.

Concentrations of particles with diameters between 12.5 and 180 nm were measured both upstream and downstream of the concentrator with the scanning mobility particle sizer (SMPS Model 3936, TSI, Inc., St. Paul, MN). The measurements were repeated at least 3 times, and the average concentration enrichment was determined as a function of particle size. The ideal enrichment factor was calculated from the ratio of the total flow entering the concentrator to the minor flow pulled from the concentrator. The actual enrichment factor was calculated from the ratio of the upstream concentration to the downstream concentration for a particular particle size.

Volatilization Loss Test

Sampling of atmospheric ultrafine aerosols under a high vacuum, such as that necessary to separate them in the Nano-MOUDI, is a concern as it might lead to evaporative losses of labile species from the collected PM. This concern, however, is not as severe as it would be when sampling particles of the accumulation mode, considering that very few volatile compounds are expected to be found in the ultrafine PM size range. This is because the vapor pressure of any species becomes much higher over the particle surface with decreasing particle size(Friedlander 1977). In order to verify the suitability of using the Nano-MOUDI for sampling and collection of semivolatile species under reduced pressure, controlled laboratory experiments were performed using artificially generated ammonium

nitrate aerosols. Preloaded aluminum foil disks (serving as impaction substrates) with varying amounts of ammonium nitrate were placed in the lowest stage of the Nano-MOUDI (having a 10 nm cut point) with sampled dry, clean air under reduced pressure for approximately 3 h. The change of mass with time was gravimetrically determined to estimate the possible evaporation loss of nitrate. Wang and John (1988) followed a similar approach to investigate the evaporation loss of nitrate from the Berner low pressure impactor. The lowest impaction stage was chosen as a test stage since it gives the lowest pressure among all the stages of Nano-MOUDI; thus it represents a worst-case scenario for losses of volatile compounds from particles collected by the Nano-MOUDI.

Polydisperse ammonium nitrate aerosols were generated by nebulization with a mass median diameter in the range of 0.04 to 0.06 μm. The size distribution of the generated aerosols was verified by the SMPS. The Nano-MOUDI sampled for a few minutes that were sufficient to collect particle mass loadings varying from about 12 to 45 μg on the 47 mm aluminum foil disks serving as impaction substrates of the 10 nm cut-point stage. The aluminum foil disks were carefully pre- and post-weighed using a Mettler Microbalance (MT5, Mettler-Toledo, Inc, Highstown, NJ). Line markers were left before disassembling the Nano-MOUDI, both on the loaded substrate and corresponding impaction stages, in order to ensure exact alignment between the loaded deposits and the corresponding impaction jets upon reassembling the sampler to conduct the evaporation tests that followed loading. The preloaded aluminum substrates with ammonium nitrate were subsequently placed in the lowest stage of the Nano-MOUDI and sampled dry, particle-free air for 3 h. This experimental duration was chosen because it corresponded to the maximum sampling period of the field tests, which will be discussed in subsequent paragraphs. The nominal flow rate of 10 l min^{-1} through the Nano-MOUDI created a pressure drop of 88 kPa (355 in. of H_2O) at the lowest stage. Experiments were interrupted every 15 or 30 min and the substrates were weighed by a microbalance (Mettler-Toledo Inc., Highstown, NJ) to determine any possible change of mass on the substrate. An unloaded aluminum substrate was used as a laboratory blank. In addition, a 47 mm aluminum foil disk was placed as an impaction substrate in the 18 nm cut-point stage of the Nano-MOUDI and was used as a "field" blank when particle-free air was sampled. Laboratory and field blanks were weighed every time the preloaded substrate was weighed. The uncertainty at the 95% confidence level did not exceed the range of ± 1 μg due to blank variability, thereby ascertaining experimental stability during these tests.

In order to compare the volatilization losses of ammonium nitrate from the lower stage of the Nano-MOUDI to those from PM collected on filters under the same vacuum, a second set of experiments was conducted in which ammonium nitrate particles were loaded on 47 mm Teflon filters (2 μm pore, PTFE Teflon, Gelman Science, Ann Arbor, MI). The preloaded Teflon filters were subsequently placed in an open-faced filter holder and tested for the evaporation loss of ammonium nitrate. The experimental conditions and procedures were otherwise identical to those followed for determining volatilization losses in the Nano-MOUDI substrates. A pressure drop of 88 kPa was created upstream of the filter by means of a small needle valve to match the pressure drop of the 10 nm stage of the Nano-MOUDI. Temperature and RH inside the laboratory throughout all of the experiments were maintained around 22°C and 40%, respectively. Similarly to the Nano-MOUDI tests, the Teflon filters were weighed in a Mettler 5 microbalance every 15–30 min to determine losses due to volatilization of ammonium nitrate.

Field Tests

This section should be prefaced with the supposition that these experiments are by no means intended to comprehensively explain ultrafine PM and their characteristics in the Los Angeles basin, but only to demonstrate how this technology can be used for future indepth characterization of this PM mode. Two series of field experiments were conducted in 2 different locations of the Los Angeles Basin. The first set of field tests was conducted in Downey, in central Los Angeles, and the second series was conducted in Riverside, CA. The locations of the field tests were chosen because each is believed to have different ambient aerosol characteristics at different times of the day. The Downey site is just east (hence downwind) of the I-710 freeway, which contributes high concentrations of diesel emissions due to heavy truck traffic. The Riverside site is upwind of the surrounding freeways, but the area has high concentrations of ammonium nitrate due to livestock and farming. Also, the aged particulate plume generated by the millions of vehicles mostly west of downtown Los Angeles is blown by the westerly winds from Los Angeles to Riverside (Allen et al. 2000). Thus, Downey is considered a "source" site, impacted primarily by relatively fresh PM emissions, while Riverside is considered a "receptor" site, in which the aerosol consists of particles generated by secondary photochemical reactions as well as those that reach this area, originally emitted in central Los Angeles (i.e., about 70 km west), after aging for several hours in the atmosphere (Pandis et al. 1992).

Tests in each site were conducted consecutively for a 6 day period between March 12 and 29, 2001. This was also a period of remarkably stable weather conditions, even by the standards of the near-ideal climate of Los Angeles. There was no precipitation or even cloud cover during any of the days of these experiments. The temperature and RH conditions in each location and during every day were virtually identical. Three time intervals—7–10 a.m., 11–2 p.m., 3–6 p.m. Pacific Standard Time (PST)—were selected in order to divide the day into periods in which different sources exist. The first interval represents the morning rush hour traffic emissions. The second interval represents the midday period, whereas the third could be dominated by evening traffic emissions and/or atmospheric chemistry, depending upon the location and conditions.

The MOUDI and Nano-MOUDI were loaded with 47 mm baked aluminum disk substrates with no after-filter employed.

A condensation particle counter (CPC Model 3022A, TSI, Inc., St. Paul, MN) measured the ambient and concentrated particle concentrations every 30 min during sampling.

Before each field experiment, the aluminum substrates were weighed with a microbalance (MT 5, Mettler-Toledo Inc., Highstown, NJ) that had a resolution of ± 1 μg. The room's temperature and humidity remained at 21–24°C and 40–50%, respectively. Aluminium foil disks were weighed twice in order to increase precision. If the balance recorded a difference of more than 2 μg between consecutive weighings, the filter was reweighed until 2 consecutive weighings differed by <3 μg. The reduction of possible sample contamination was achieved by storing all collection media in sterile Petri dishes sealed with Teflon tape both before and after sampling. All samples were stored in a freezer at -10°C until being sent for laboratory analysis. At the end of each experiment, the aluminum disks were weighed again after a 24 h equilibration period in the same controlled temperature and RH laboratory to determine the collected mass in each Nano-MOUDI stage. Subsequent to weighing, the substrates were divided into 2 pieces so that they could be analyzed by 2 different methods. The smaller piece ($\sim$0.2 cm^2) of each aluminum substrate was subjected to thermo-analysis for determination of elemental and organic carbon (EC/OC) using a method described in greater detail by Fung (1990). The remainder of the substrate was extracted with 3 mL of ultrapure deionized water and analyzed via ion chromatography to measure the concentration of nitrate (NO_3^-) and sulfate (SO_4^{2-}). Based on a sampling air volume of 39.6 m^3 in each field run, the lowest detectable concentrations, defined as 3 times the limit of detection of the analytical method used, obtained for mass, EC, OC, nitrate, and sulfate were 100, 2, 2, 15, and 17 ng/m^3, respectively.

RESULTS AND DISCUSSION

Laboratory Tests

Figure 2 displays the graph of the concentration enrichment versus aerodynamic particle diameter for the 3 aerosol types. Due to the limitation of the specific SMPS used in these experiments, the concentrations of particles with diameters smaller than 12 nm could not be measured. The average enrichment factors for particles in the 12–180 nm range obtained for indoor air, ammonium nitrate, and ammonium sulfate were 19.7 ($\pm$1.3), 20.6 ($\pm$1.5), and 19.4 ($\pm$1.4), respectively. As evident from the results plotted in Figure 2 as well as the determined standard deviations in the enrichment factors, the concentration enrichment is uniform across the entire particle size range from 12 to 180 nm and very close to its ideal value of 22. The ability to enrich the concentrations of ultrafine particles without any distortion in the original size distribution of the ambient aerosol is a

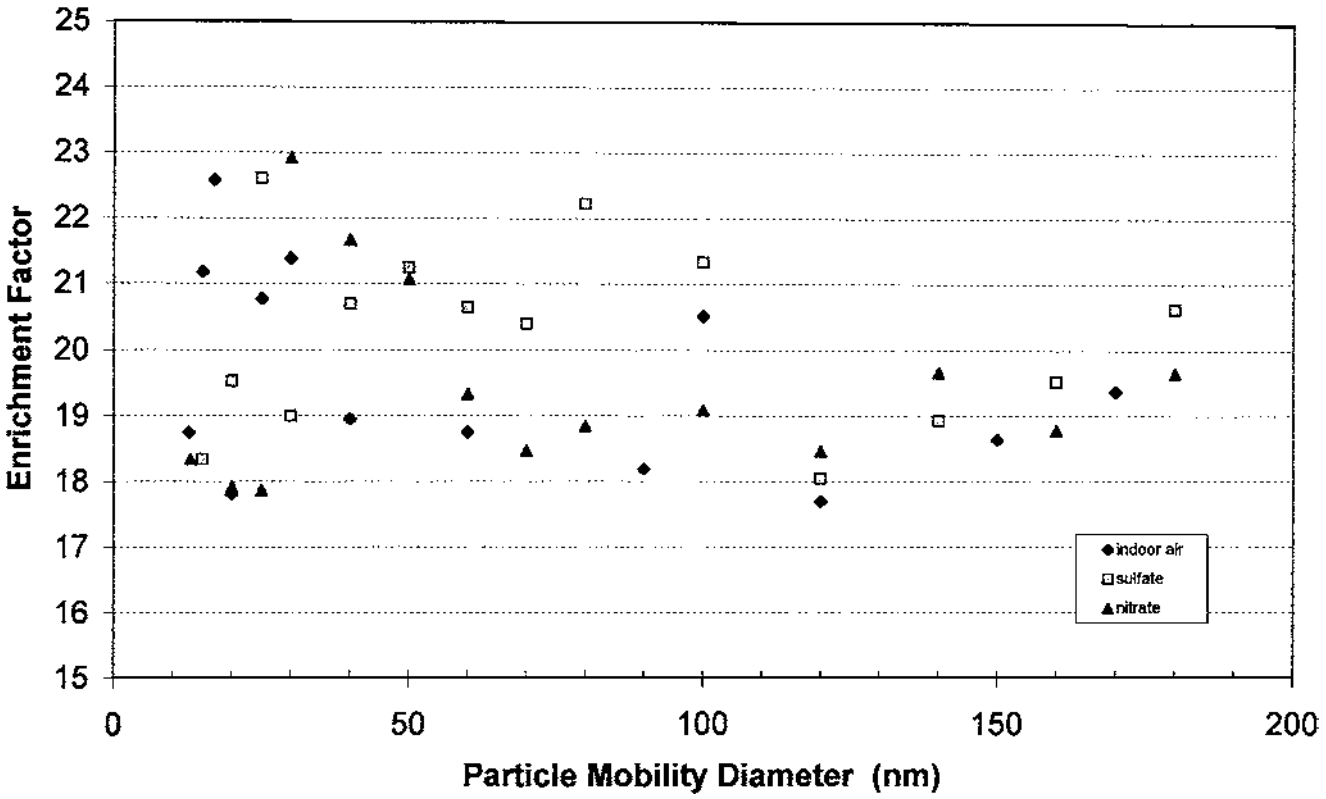

Figure 2. Laboratory characterization of the Ultrafine Concentrator using indoor aerosols as well as ammonium sulfate and ammonium nitrate aerosols.

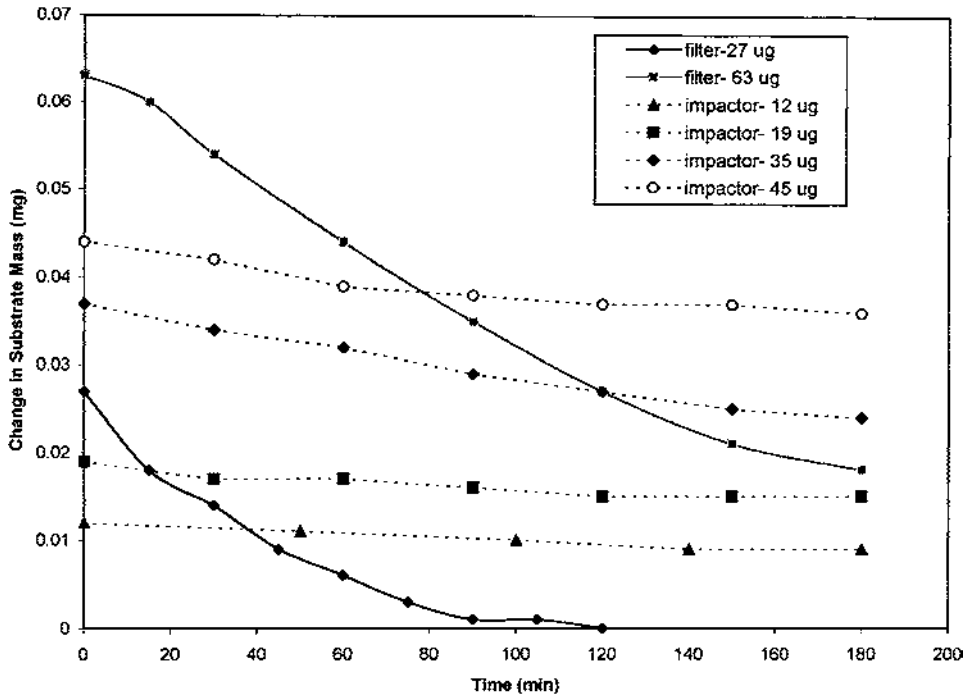

Figure 3. Ammonium nitrate losses due to volatilization from the Nano-MOUDI and Teflon filter substrates as a function of time and for different particle loadings.

very important attribute of the ultrafine concentrator technology that was used in this study. The data plotted in Figure 2 further indicate that the concentration enrichment values obtained for ammonium nitrate particles is practically identical to that observed for nonvolatile ammonium sulfate and the real-life indoor air particles, which are comprised mostly of hydrophobic compounds such as OC and EC (Kim et al., 2000b). These results suggest that particle properties, such as hygroscopicity and volatility, do not seem to affect the degree to which these particles are concentrated by this technology. A substantially more detailed chemical characterization of the PM concentrated by this system and their relation to those of ambient ultrafine PM is presented elsewhere (Kim et al. 2001a,b). Briefly, these studies have unequivocally shown that the concentration enrichment process does not differentially affect the particle chemical composition (i.e., nitrate, sulfate, EC, OC, trace element, and metal content) or even themorphological properties of ambient ultrafine PM.

Volatilization Loss Test

Results from the ammonium nitrate volatilization tests from the Nano-MOUDI and filter samplers operating under reduced pressure are shown in Figure 3. Figure 3 shows the decrease in ammonium nitrate mass as a function of time of exposure to particle-free air for the 2 samplers (i.e., Nano-MOUDI, filter) and with different initial nitrate mass loadings.

One of the most striking features of the data plotted in Figure 3 is the substantial difference in the rate of volatilization of ammonium nitrate from impactor substrates and filters under the same reduced pressure. Based on the results shown in Figure 3, the volatilization rate from filters is approximately 20 μg of ammonium nitrate per hour and is relatively independent of the initial mass loading. By comparison, losses of ammonium nitrate from the last stage of the Nano-MOUDI seem almost negligible, at least over the 3 h period of exposure to particle-free air passing through the sampler at 10 l min^{-1}. Nitrate losses from the 10 nm Nano-MOUDI stage range between 2 and 5 μg of the original loading and in general do not seem to be dependent upon the actual mass loading.

Similar observations were made by Wang and John (1988), who reported that evaporation loss of ammonium nitrate from impactor substrates was not as significant compared to that from filters, primarily due to the much smaller deposit area per unit mass of particulate matter of impactors compared to filters. Particle collection in a 47 mm Teflon filter occurs over a surface area of about 14 cm^2. Assuming that the diameter of the particulate deposit in an impactor is roughly 1.5 times the diameter of the acceleration jet (Zhang and McMurry 1987), and considering that the last Nano-MOUDI stage consists of 2000 jets, each 0.005 cm in diameter (Table 1), the estimated particulate deposit area of the 10 nm cut point Nano-MOUDI stage is 0.088 cm^2, thus about 160 times smaller than that of a 47 mm filter. Furthermore, while in filters the air flows through the filter and around its fibers and thus comes in closer contact with the collected particles, the stagnation boundary layer that forms naturally around the particulate deposit area in laminar flow impactors, such as

those of the Nano-MOUDI (Biswas et al. 1987),tends to further reduce the contact zone between the air streamlines and collected particles. The combination of these 2 factors (i.e., reduced surface area and formation of a stagnation flow boundary layer) results in lower losses of volatile species from PM collected in impactors compared to filters. In addition to the present study and that by Wang and John (1988), similar observations corroborating the lower losses of impactors were made by Chang et al. (2000) and Zhang and McMurry (1992).

RESULTS FROM FIELD TESTS

Downey

Ambient particle concentrations averaged $2.3 \times 10^4 \pm 6.9 \times 10^3$ particles/cm^3 in the morning and $2.3 \times 10^4 \pm 4.6 \times 10^3$ in the midday time slot, while increasing to $2.9 \times 10^4 \pm 6.7 \times 10^3$ particles/cm^3 in the afternoon hours. The enriched concentrations measured downstream of the USC Ultrafine Concentrator ranged from 3.3 to 6×10^5 particles/cm^3, respectively.

The average mass concentrations of PM with aerodynamic diameters between 10 and 320 nm at Downey were 3.97, 2.67, and 1.98 μg/m^3 for morning, midday, and afternoon, respectively. Of these, the average ultrafine (10–100 nm) mass concentrations were 1.92, 0.88, and 0.81 μg/m^3, respectively. Figure 4a displays a distinct mode in the 32–56 nm size range of ultrafine PM that is independent of time of the day.

Despite its location downwind of a freeway with relatively constant heavy-duty traffic, ultrafine PM mass concentration at Downey is highest in the morning and lowest in the afternoon. This is most likely due to the combination of increasing wind velocity and atmospheric mixing depth as well as the declining vehicular source contributions as the day progresses, and this is demonstrated by the overall decrease in mass concentration

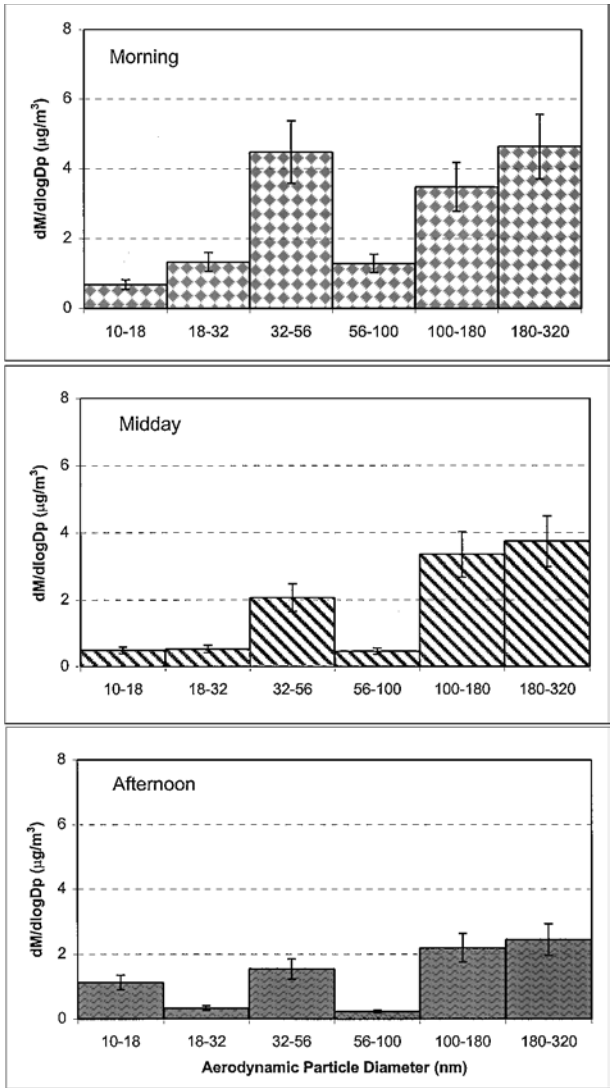

(a)

Figure 4. Variation of daytime ultrafine PM concentrations at Downey for (a) mass, (b) OC, (c) EC, (d) nitrate, and (e) sulfate. *(Continued)*

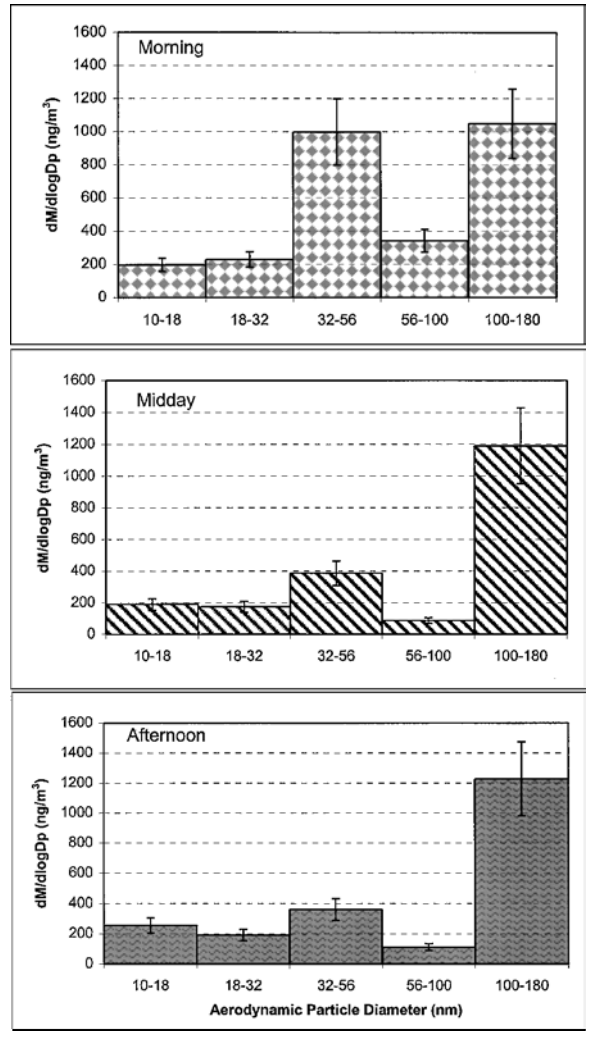

(b)

Figure 4. (Continued)

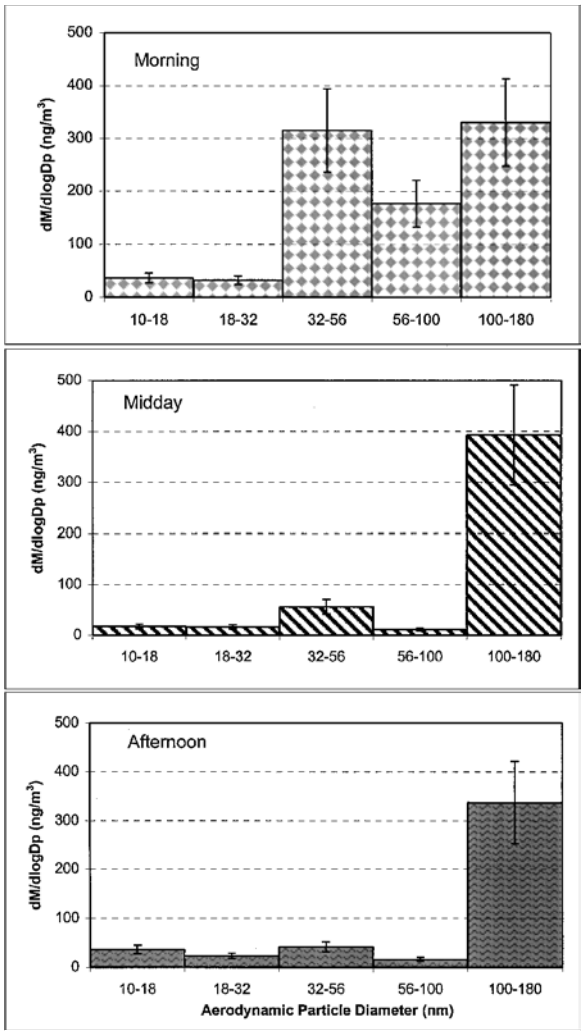

(c)

Figure 4. (Continued)

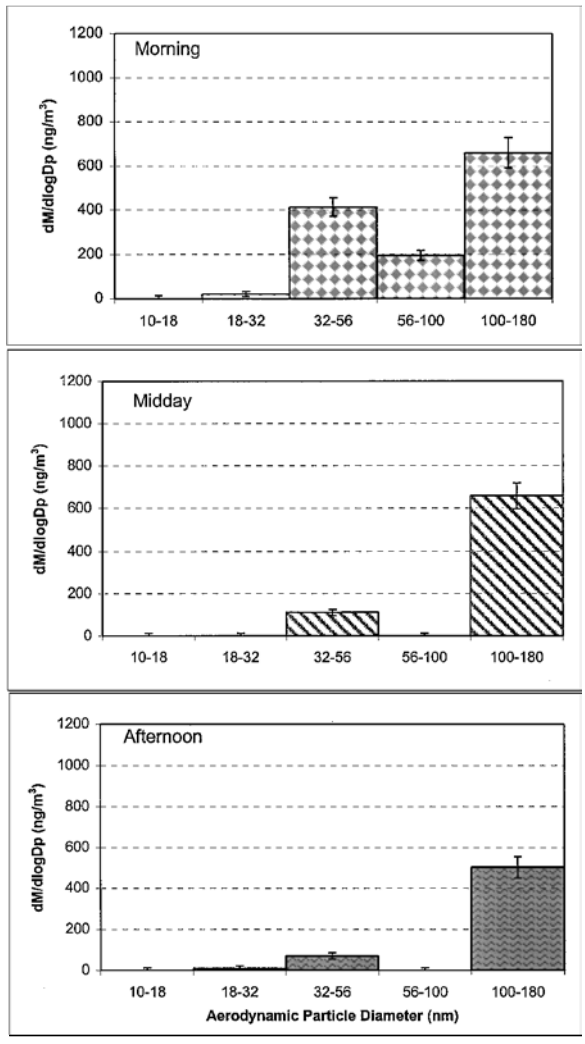

(d)

Figure 4. (Continued)

throughout the day in Figure 4a. Furthermore, the shape of the mass-based size distribution curves obtained for the 3 time intervals remains relatively constant during the day, which reaffirms that Downey is a "source" site.

Since the primary source of atmospheric ultrafine PM at Downey is the 710 freeway, which is characterized by both heavy diesel and gasoline engine traffic, the mass-based size distribution is expected to be driven by the OC-based size distribution. This is the case for all 3 time intervals. The notable difference between the midday and the morning time periods is the large reduction in the 32–100 nm range of OC, particularly in the 32–56 nm range, while the other sizes remain quite unaffected (Figure 4b). The increased concentrations in the 32–56 nm mode during the morning period may be due to particle formation in that size range by means of condensation of organic vapors emitted by both automobile and truck vehicles. The lower ambient temperatures and higher RHs during this time period, combined with the low mixing depth of the atmosphere, favor the formation of particles from condensable organic vapors. Our findings are further corroborated by previous studies by Kittelson (1998) and Tobias et al. (2001), which have shown that the mass-based size distribution of particles from diesel exhaust display a bimodal structure, with a so-called nuclei mode having a mass median diameter (MMD) in the 30–60 nm range and an "accumulation mode" with a MMD in the 100–200 nm range. The nuclei mode generally consists of mainly volatile materials, whereas the accumulation mode generally consists of solid carbonaceous particles. The formation mechanisms proposed for this nucleation submode involve homogeneous binary nucleation of sulfuric acid generated by oxidation of sulfur in diesel, followed by growth from condensation of organic species (Shi and Harrison 1999; Kittelson 1998).

The size distribution of EC closely follows that of the total mass, with the most deviation occurring in the morning when the primary sources of EC presumably contribute the most. Figure 4c shows the abundance of EC in the morning, which

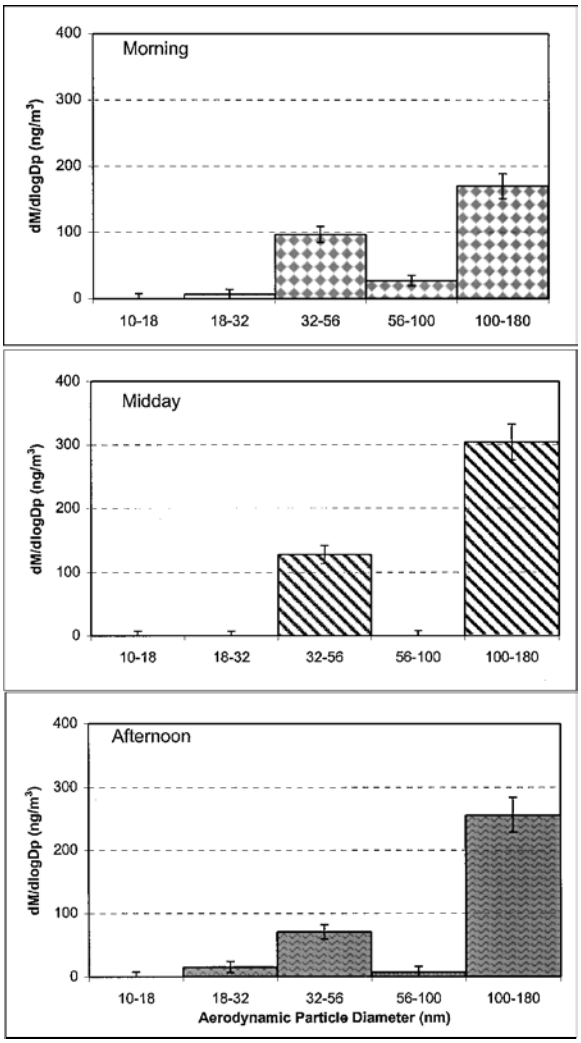

(e)

Figure 4. (Continued)

most likely occurs due to the combined effects of overnight and early morning accumulation of the emissions from the steady truck traffic and the depressed atmospheric mixing depth. The concentrations quickly drop as the mixing depth increases and traffic sources trail off slightly during the day. EC is barely present in the lower size ranges because it has a mode of 100 nm and quickly diminishes in size ranges that vary in either direction (Seinfeld and Pandis 1998). The emission profile of diesel vehicles, which contain high proportions of EC, further reinforces this concept (Durbin et al. 1999; Tobias et al. 2001).

Figures 5a–c illustrate the excellent correlation between EC and OC for all 3 time periods at Downey. The slopes of the regression lines provide an average estimate of the OC-to-EC concentration ratio. The coefficient of determination (R^2) for each time interval is 0.90–0.94 with the slope of the line decreasing throughout the day. OC concentrations are approximately 2.4 times those of EC in the morning, 2.7 times during midday, and 3.4 times that of EC in the afternoon. This trend points to a decline in EC or an escalation of OC concentrations as the day progresses. The high correlation between EC and OC in Downey implies that OC is generated mostly by primary emissions and not as much by secondary gas-to-particle formation reactions. However, these secondary reactions along with photochemistry still may cause the increase in the ratio as the day progresses. The OC-to-EC ratios measured in mostly diesel engines either directly (e.g., in a dynamometer facility) or indirectly in road tunnels varied from 1–3 (Fraser et al. 1999; Hildemann et al. 1991), and thus were close to the range of the reported values at Downey. It should be noted that studies of gasoline and diesel vehicles measured all fine mass and not just the 0–320 nm diameter particle mass. The ratios mentioned above are around the 1–3 range but may differ from this because of the exclusion of fine particles above 320 nm from this study.

As shown in Figure 4d, the amount of particle-bound nitrate in Downey decreases all through the day. As with the other chemical constituents and the total mass distributions, a minimum can be observed in the 56–100 nm range. Nitrate is probably decreasing throughout the day due to the increasing temperature and decreasing RH, both of which cause the particle-gas phase nitrate equilibrium to shift from the particulate to gaseous form (Mozurkewich 1993).

Figure 4e illustrates the daytime variation of particulate sulfate in Downey. Ultrafine PM sulfate displays a bimodal distribution, with measurable amounts in the 32–56 and 100–180 nm ranges. The 32–56 nm mode originates probably from sulfur contained in diesel vehicular emissions, as discussed in the previous paragraph, whereas the 100–180 nm mode is mostly generated by photochemical oxidation of sulfur dioxide (SO_2) to sulfate during the midday and afternoon (Shi and Harrison 1999). These 2 different formation mechanisms may explain the decrease of sulfate in the 32–56 nm mode (i.e., the decrease in traffic and increase in atmospheric mixing depth) and the increases in the 100–180 nm modes as the day progresses.

Riverside

Ambient particle concentrations averaged 1.1×10^4 particles/cm^3 in the morning, 9.3×10^3 particles/cm^3 at midday, and 1.0×10^4 particles/cm^3 in the afternoon hours. The average enriched concentrations measured downstream of the USC Ultrafine Concentrator were 2.2, 1.9, 2.0, $\times 10^5$ particles/cc, respectively.

The average mass concentrations of PM with aerodynamic diameters between 10 and 320 nm at Riverside were 2.58, 2.22, and 3.65 μg/m^3 for morning, midday, and afternoon, respectively. Of these, the average ultrafine (10–100 nm) mass concentrations were 0.76, 0.65, and 0.80 μg/m^3, respectively. Figure 6a displays a much less pronounced mode in the 32–56 nm size range of ultrafine PM when compared to that of Downey.

Because Riverside is a receptor site, the highest mass concentrations are found in the afternoon, while midday concentrations are the lowest. The decline at midday is most likely due to

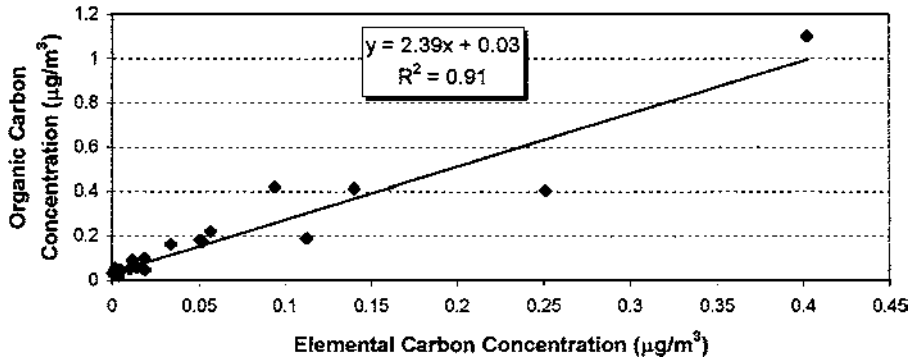

(a)

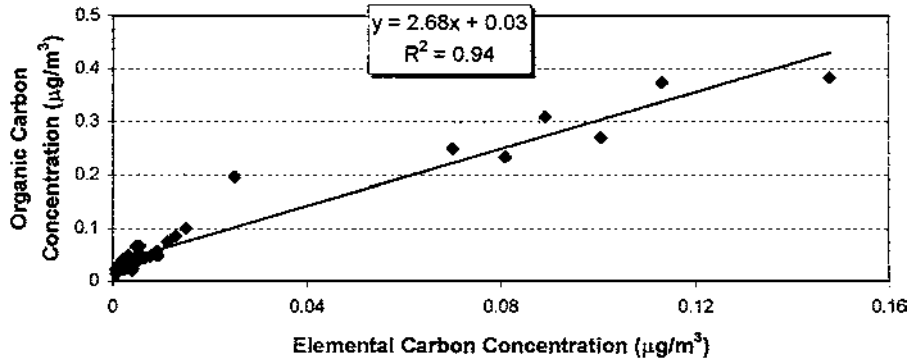

(b)

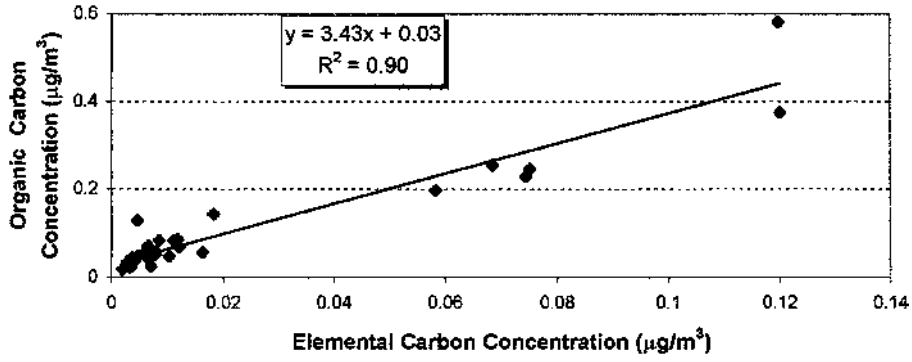

(c)

Figure 5. EC versus OC ultrafine PM concentrations in Downey: (a) morning; (b) midday; and (c) afternoon.

a combination of increasing wind velocity and mixing depth as the day progresses. The afternoon concentrations, however, peak because of secondary particle formation through photochemical reactions occurring during the warmest part of the day (Pandis et al. 1992). While the morning and midday size distributions remain fairly constant, with mass concentration decreasing with time, the afternoon distribution differs from these in both shape and intensity. The most notable difference is the surge in the 100–180 nm particle range in the afternoon, which may occur because of photochemical secondary aerosol formation, progression of the urban Los Angeles plume from west to east, and/or growth of ultrafine particles. The latter mechanism is rather unlikely given that RH, which may have caused ultrafine particle growth, is at a minimum during this time of the day. The first 2 mechanisms, however, are equally likely, and the discussion in the following paragraphs, including the size-fractionated chemical composition of ultrafine PM in Riverside, will illustrate the relative importance of each.

The OC size distribution (Figure 6b) is very similar to that of total mass; as with Downey, OC is the predominant chemical

constituent of ultrafine PM at Riverside, accounting for approximately 50–80% of the total mass. The peak in the 32–56 nm range is less pronounced at Riverside and is only distinguishable during the morning period, probably due to the contribution of vehicular emissions. OC concentrations in the 100–180 nm size range increase in the afternoon after dropping off at midday.

Figure 6c shows that EC concentrations are very small in the ultrafine mode for all time periods at Riverside, which demonstrates the lack of overnight and morning diesel emissions in that location compared to Downey. The majority of the EC at Riverside is associated with the 100–180 nm mode, thereby displaying a very similar size distribution with particle-bound EC typically measured in diesel engine exhaust (Durbin et al. 1999; Tobias et al. 2001; Shi and Harrison 1999). This is because vehicular emissions are still the main sources of EC found in ultrafine PM at Riverside, but the lower concentrations are due to the overall lower traffic in that region compared to that of downtown Los Angeles. EC concentrations become maximum during the morning traffic period. Once the atmospheric mixing depth increases after the morning hours, the EC concentrations drop and remain constant from midday to afternoon. This diurnal pattern suggests that there are no significant contributions to the EC levels measured in Riverside that could be attributed to the urban plume of Los Angeles, which would have increased the afternoon concentrations. Thus the increased ultrafine PM mass and OC concentrations measured in Riverside during that period must be attributed to secondary aerosol

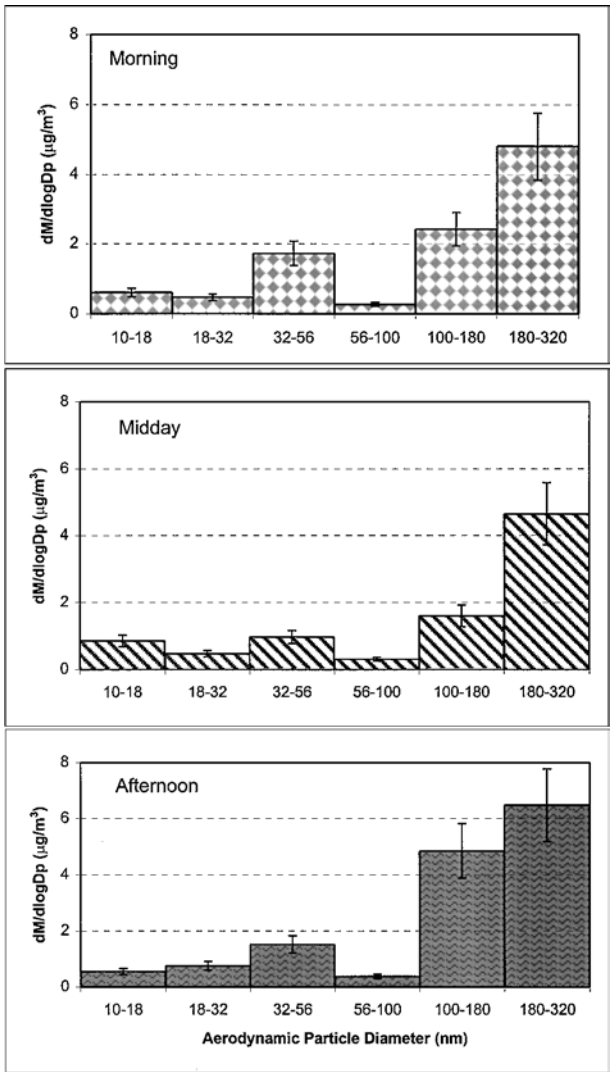

(a)

Figure 6. Variation of daytime ultrafine PM concentrations at Riverside for (a) mass, (b) OC, (c) EC, (d) nitrate, and (e) sulfate. *(Continued)*

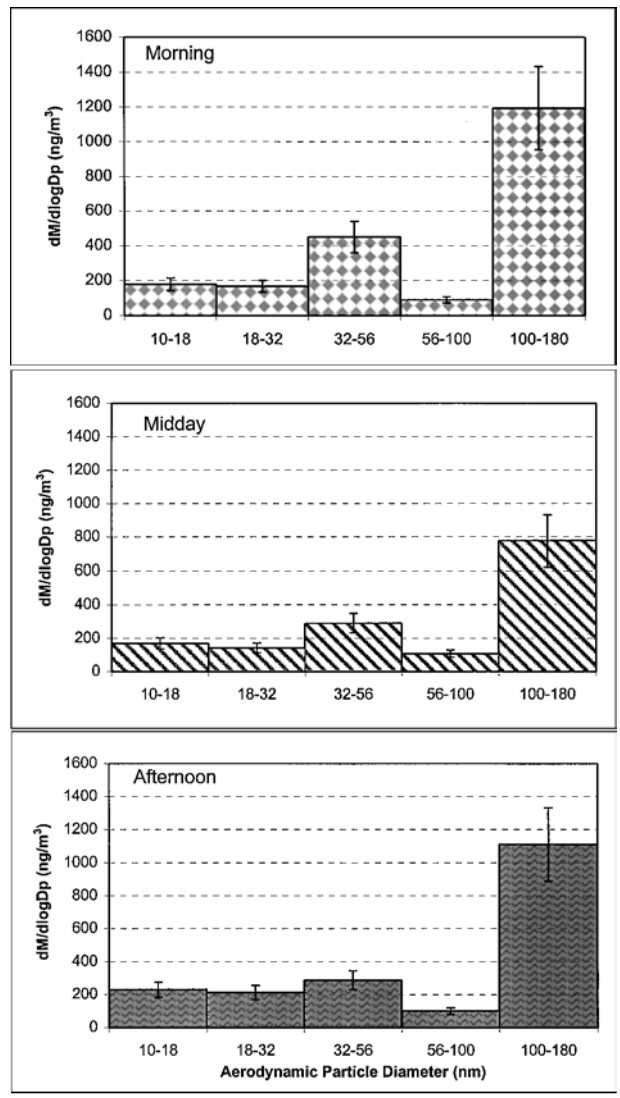

(b)

Figure 6. (Continued)

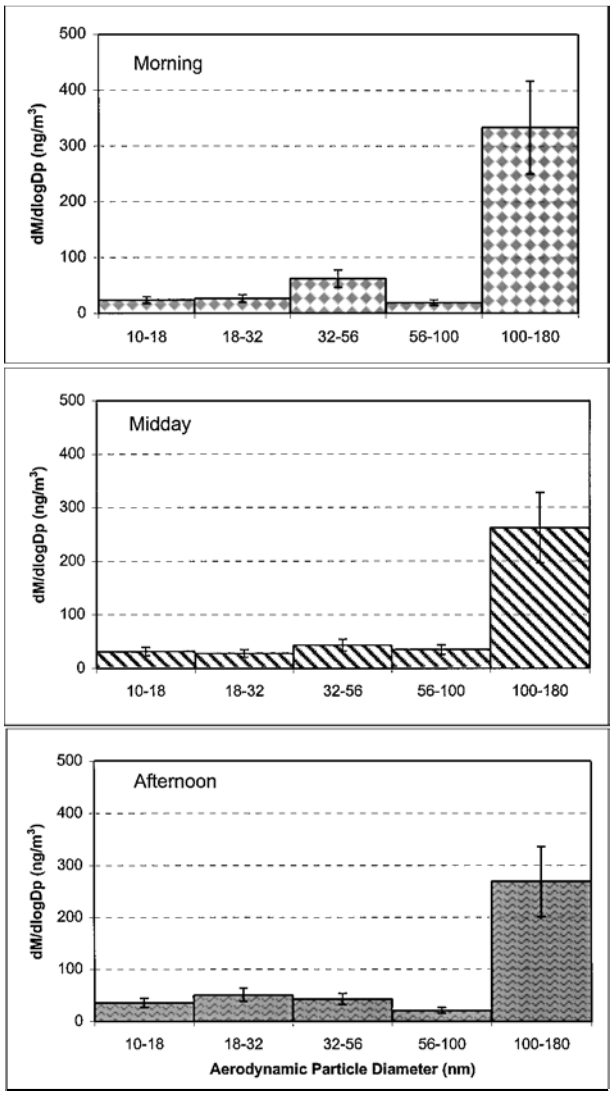

(c)

Figure 6. (Continued)

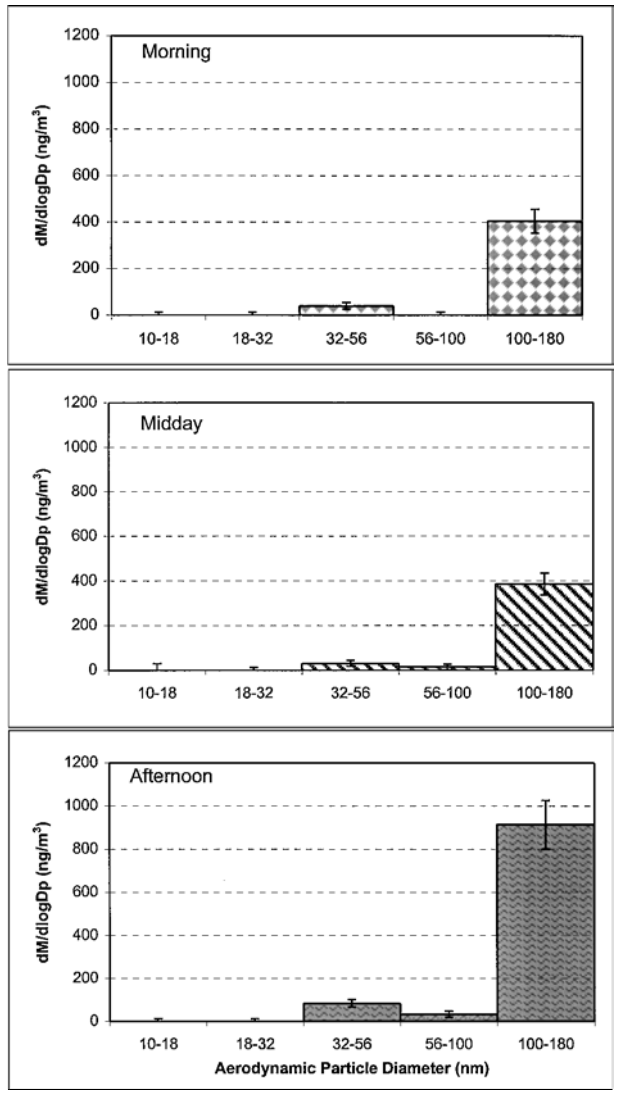

(d)

Figure 6. (Continued)

formation. This conclusion is further corroborated by the plots of the EC versus OC concentrations in Riverside for different time periods, shown in Figures 7a–c. Figure 7a illustrates a very high correlation ($R^2 = 0.90$) between EC and OC concentrations in the 10–100 nm range for the morning traffic period at Riverside, thereby suggesting that at that time vehicular emissions are the predominant contributors to ultrafine PM mass and OC. This correlation between the EC and OC data collapses as the day progresses, with R^2 decreasing to 0.13 and 0.25 in midday and afternoon, respectively, thereby suggesting that a very substantial fraction in the variability of the OC concentration cannot be explained by primary emissions. Increased secondary organic aerosol formation during the early afternoon hours in the eastern ("receptor") regions of the Los Angeles Basin has also been observed in previous studies (Pandis et al. 1992; Turpin and Hutzincker 1995).

Also noteworthy are the higher ratios of OC to EC in Riverside compared to Downey, averaging 7.5, 9.9, and 7.5 for morning, midday, and afternoon periods. The increased OC to EC ratio in the afternoon is mostly due to the increase in secondary organic aerosol formation at that time. The increased OC to EC ratio during the morning hours (the only time of day during which primary emissions seem to be the main sources of organic PM) indicates that gasoline engine emissions may be more significant primary sources of ultrafine PM in Riverside when compared to Downey.

Further evidence of increased secondary aerosol formation in the Riverside area compared to Downey is provided by examining the diurnal trends in the concentrations of particulate-bound nitrate, as shown in Figure 6d. Particulate nitrate in Riverside is almost exclusively found in particles larger than 100 nm, and its concentrations increase throughout the day, which is exactly

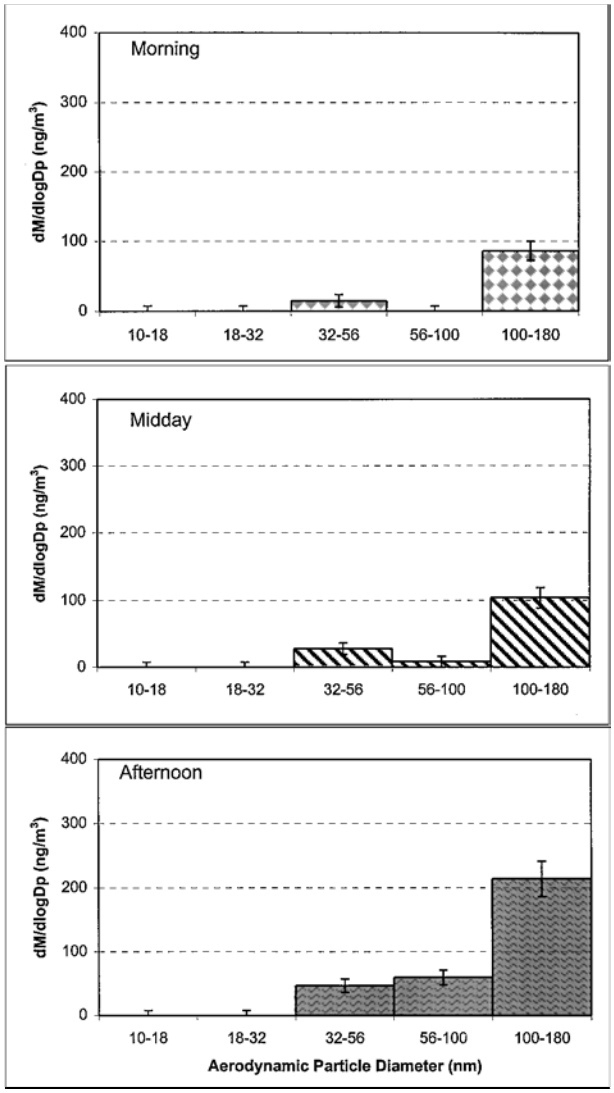

(e)

Figure 6. (Continued)

the opposite trend of that in Downey. Unlike Downey, Riverside is located a few kilometers downwind of major ammonia sources generated by local agriculture and dairy farms(Kleeman et al. 1999). Previous studies have indicated that as air parcels originating from downtown Los Angeles are advected inland and the nitric acid carried by these parcels mixes with theseammonia sources (typically in early afternoon), a large production of ammonium nitrate results (Allen et al. 2000). This increased ammonia is enough to overcome the high temperature and low humidity effects during midday and afternoon hours, which would impede nitrate formation. Riverside nitrate concentrations surpass those of Downey in the afternoon.

The particle-bound sulfate concentrations, shown in Figure 6e, increase from morning to afternoon similarly to the particulate nitrate concentrations. Similar to the results observed in Downey, small but measurable amounts of sulfate were found in the 32–56 nm mode. Given that the concentrations in this submode increase as the day progresses (and opposite to Downey), we hypothesize that they probably originate from diesel emissions from the urban areas of Los Angeles, especially given the lack of sulfate emissions in Riverside (Kimet al. 2000a). The majority of sulfate was found in the 100–180 nm range, hence the "tail" of the accumulation PM mode. It should be noted that the levels of ultrafine PM-bound sulfate are much lower than those of nitrate in Riverside. Also notable is that Riverside sulfate levels are never greater than those at Downey, even in the afternoon, most likely due to the lack of a sulfate source in Riverside.

SUMMARY AND CONCLUSIONS

This study demonstrates the use of a technology that can collect size-segregated, ambient ultrafine PM on substrates that can be further analyzed for chemical speciation. By concentrating ambient ultrafine aerosols at 2 locations in southern California before entering a cascade impactor under vacuum, concentrations as low as 0.1 $\mu g/m^3$ can be detected for time periods on the order of 3 h. Because of the localization of ultrafine PM and the brevity of events and mechanisms that might be responsible for its formation, sampling over shortened intervals has greater practicality than the traditional 24 h sampling experiments. Although the results presented in this paper provide new insight into ultrafine PM formation mechanisms in locations of the Los Angeles Basin that are impacted by either primary or secondary aerosol formation processes, they are not intended to comprehensively explain ultrafine PM and its characteristics. This technology can, however, be duplicated at various locations and times in order to develop a comprehensive understanding of the formation mechanisms, transport, and transformations of ultrafine particles.

The ultrafine aerosol concentration enrichment by a factor of over 20 allowed for a size-fractionated collection of weighable and analyzable amounts of ultrafine PM in 5 ranges from 10 to 180 nm in 3 h sampling periods. Despite the rather limited number of sampling days, substantially different trends in the size distributions and diurnal trends for mass and chemical constituents were observed between the 2 sampling sites, thereby providing insights into differences in the ultrafine particle formation processes in each location. At Downey, a "source" site, impacted primarily by vehicular emissions of nearby freeways, very strong correlations were obtained for particulate EC versus OC throughout the day. In Riverside, a "receptor" site in the Los Angeles Basin, ultrafine EC and OC concentrations were highly correlated only during the morning period, whereas these correlations collapsed later in the day. These results indicate that in this area, ultrafine PM are generated by primary emissions during the morning hours, whereas secondary aerosol formation processes become more important as they day progresses.

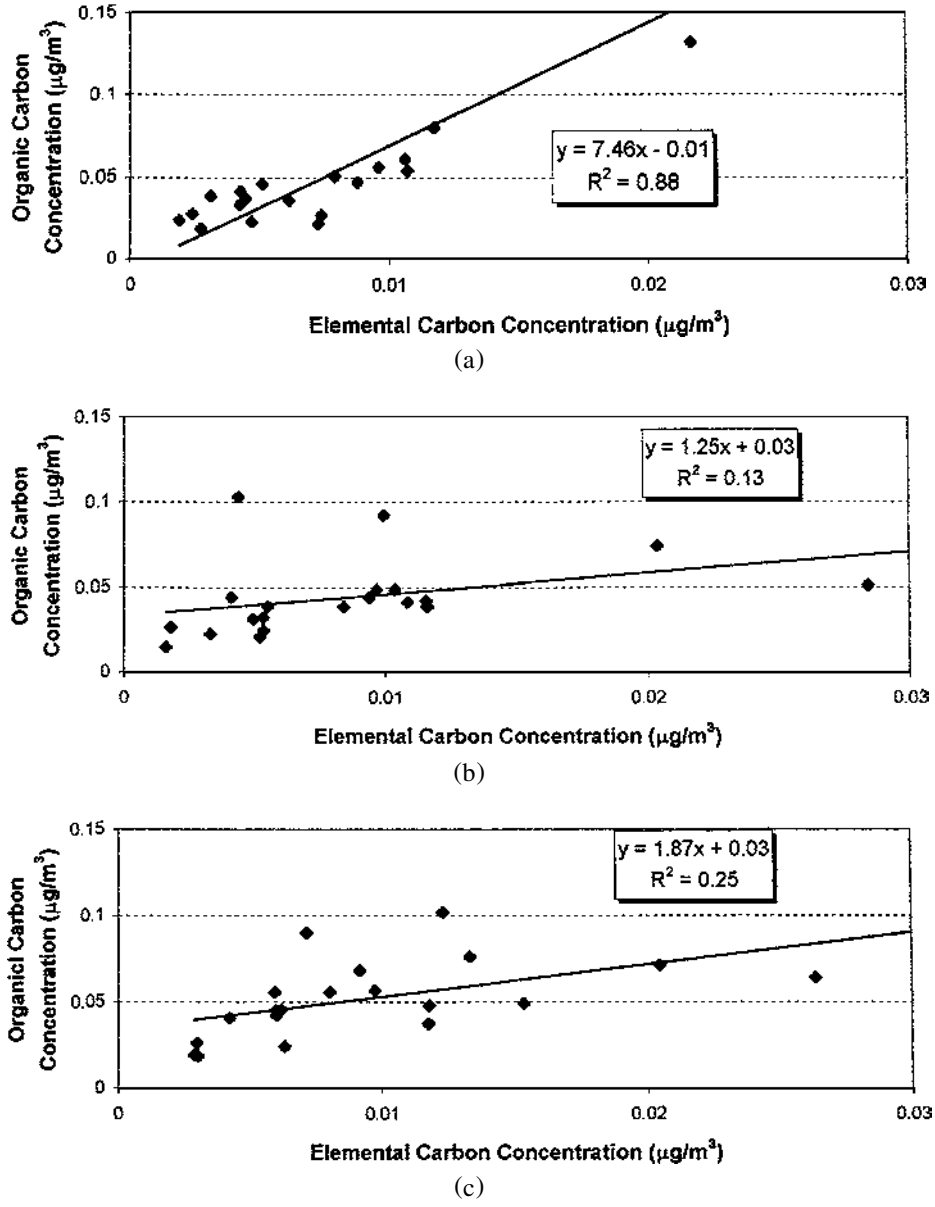

Figure 7. EC versus OC ultrafine PM concentrations in Riverside: (a) morning; (b) midday; and (c) afternoon.

REFERENCES

Allen, J. O., Hughes, L. S., Salmon, L. G., Mayo, P. R., Johnson, R. J., and Cass, G. R. (2000). *Characterization and Evolution of Primary and Secondary Aerosols during $PM_{2.5}$ and PM_{10} Episodes in the South Coast Air Basin*, Report A-22 to the Coordinating Research Council (CRC).

Biswas, P., Jones, C. L., and Flagan, R. C. (1987). Distortion of Size Distribution by Condensation and Evaporation in Aerosol Instruments, *Aerosol Sci. Technol*. 7:231–246.

Cass, G. R., Hughes, L. A., Bhave, P., Kleeman, M. J., Allen, J. O., and Salmon, L. G. (2000). The Chemical Composition of Atmospheric Ultrafine Particles, *Philosophical Transactions of the Royal Society of London A*, 358(1775):2581–2592.

Chang, M. C., Sioutas, C., Kim, S., Gong, H., and Linn, W. (2000). Reduction of Nitrate Losses from Filter and Impactor Samplers by Means of Concentration Enrichment, *Atmos. Environ*. 34:86–98.

Dockery, D. W., Pope, C. A., Xu, X., Spengler, J. D., Ware, J. H., Fay, M. E., Ferris, B. G., and Speizer, F. E. (1993). An Association between Air Pollution and Mortality in 6 United States Cities, *New England Journal of Medicine* 329:1753–1759.

Donaldson, K., and MacNee, W. (1998). The Mechanism of Lung Injury Caused by PM_{10}. In *Issues in Environmental Science and Technology*, edited by R. E. Hester and R. M. Harrison, no. 10, pp. 21–32, The Royal Society of Chemistry, London, UK.

Durbin, T. D., Norbeck, J. M., Smith, M. R., and Truex, T. J. (1999). Particulate Emission Rates from Light-Duty Vehicles in the South Coast Air Quality Management District, *Environ. Sci. Technol*. 33:4401–4406.

Fraser, M. P., Cass, G. R., and Simoneit, B. T. (1999). Particulate Organic Compounds Measured from Motor Vehicle Exhausts and in Urban Atmosphere, *Atmos. Environ*. 33:2715–2724.

Frielander, S. K. (1977). *Smoke, Dust, and Haze: Fundamentals of Aerosol Behavior*, John Wiley & Sons, Inc., New York.

Fung, K. (1990). Particulate Carbon Speciation by MnO_2 Oxidation, *Aerosol Sci. Technol.* 12:122–127.

Harrison, R. M., Shi, J. P., Xi, S., Khan, A., Mark, D., Kinnersley, R., and Yin, J. (2000). Measurement of Number, Mass and Size Distribution of Particles in the Atmosphere, *Philosophical Transactions of the Royal Society of London A* 358(1775):2567–2579.

Hildemann, L. M., Markowski, G. R., and Cass, G. R. (1991). Chemical Composition of Emissions from Urban Sources of Fine Organic Aerosol, *Environ. Sci. Technol.* 25:744–759.

Hughes, L. S., Cass, G. R., Gone, J., Ames, M., and Olmez, I. (1998). Physical and Chemical Characterization of Atmospheric Ultrafine Particles in the Los Angeles Area, *Environ. Sci. Technol.* 32:1153–1161.

Kim, B. M., Tefferra, S., and Zeldin, M. D. (2000a). Characteristics of $PM_{2.5}$ and PM_{10} in the South Coats Air Basin of Southern California: Part I–Spatial Variations, *J. Air Waste Manage. Assoc.* 50:2034–2044.

Kim, S., Chang, M. C., and Sioutas, C. (2000b). A New Generation of Portable Coarse, Fine and Ultrafine Particle Concentrators for Use in Inhalation Toxicology, *Inhal. Toxicol.* 12(1):121–137.

Kim, S., Jaques, P., Chang, M. C., Froines, J. R., and Sioutas, C. (2001). A Versatile Aerosol Concentrator for Simultaneous In Vivo and In Vitro Evaluation of Toxic Effects of Coarse, Fine and Ultrafine Particles: Part I: Laboratory Evaluation, *J. Aerosol Sci.* 11:1281–1297.

Kim, S., Jaques, P., Chang, M. C., Xiong, C., Friedlander, S. K., and Sioutas, C. (2001). A Versatile Aerosol Concentrator for Simultaneous In Vivo and In Vitro Evaluation of Toxic Effects of Coarse, Fine and Ultrafine Particles: Part II: Field Evaluation, *J. Aerosol Sci.* 11:1299–1314.

Kittelson, D. B. (1998). Engines and Nanoparticles: A Review, *J. Aerosol Sci.* 29(5–6):575–588.

Kleeman, M. J., and Cass, G. R. (1998). Source Contribution to the Size and Composition Distribution of Urban Particulate Air Pollution, *Atmos. Environ.* 32:2803–2816.

Kleeman, M. J., Hughes, L. S., Allen, J. O., and Cass, G. R. (1999). Source Contributions to the Size and Composition Distribution of Atmospheric Particles: Southern California in September 1996. *Environ. Sci. Technol.* 33:4331–4341.

Marple, V. A., and Olson, B. A. (1999). *A Micro-Orifice Impactor with Cut Sizes Down to 10 Nanometers for Diesel Exhaust Sampling*, Final Report Generic Center for Respirable Dust, Pennsylvania State University, University Park, PA.

Mozurkewich, M. (1993). The Dissociation Constant of Ammonium Nitrate and its Dependence on Temperature, Relative Humidity and Particle Size, *Atmos. Environ.* 27A:261–270.

Oberdörster, G., Ferin, J., Gelein, R., Soderholm, S. C., and Finkelstein, J. (1992). Role of Alveolar Macrophage in Lung Injury; Studies with Ultrafine Particles, *Environ. Health Perspect.* 102:173–179.

Oberdörster, G., Gelein, R. M., Ferin, J., and Weiss, B. (1995). Association of Particulate Air Pollution and Acute Mortality: Involvement of Ultrafine Particles, *Inhal. Toxicol.* 7:111–124.

Pandis, S. N., Harley, R. A., Cass, G. R., and Seinfeld, J. H. (1992). Secondary Organic Aerosol Formation and Transport, *Atmos. Environ.* 26A:2269–2282.

Pope, C. A., Dockery, D. W., and Schwartz, J. (1995). Review of Epidemiological Evidence of Health Effects of Particulate Air Pollution, *Inhal. Toxicol.* 7:1–18.

Schlesinger, R. B. (1995). Toxicological Evidence for Health Effects from Inhaled Particulate Pollution—Does it Support the Human Experience?, *Inhal. Toxicol.* 7:99–109.

Seinfeld, J. H., and Pandis, S. N. (1998). *Atmospheric Chemistry and Physics: From Air Pollution to Climate Change*, New York: John Wiley & Sons, Inc., pp. 700–751.

Shi, J. P., Khan, A. A., and Harrison, R. M. (1999). Measurements of Ultrafine Particle Concentration and Size Distribution in the Urban Atmosphere, *Sci. Total Environ.* 235(1–3):51–64.

Sioutas, C., Kim, S., and Chang, M. (1999). Development and Evaluation of a Prototype Ultrafine Particle Concentrator, *J. Aerosol Sci.* 30(8):1001–1012.

Tobias, H. J., Beving, D. E., Ziemann, P. J., Sakurai, H., Zuk, M., McMurry, P. H., Zarling, D., Waytulonins, R., and Kittelson, D. B. (2001). Chemical Analysis of Diesel Engine Nanoparticles Using a Nano-DMA Thermal Desorption Particle Beam Mass Spectrometer, *Environ. Sci. Technol.* 35:2233–2243.

Turpin, B. J., and Hutzincker, J. J. (1995). Identification of Secondary Organic Aerosol Episodes and Quantitation of Primary and Secondary Organic Aerosol Concentrations During SCAQS, *Atmos. Environ.* 29(23):3527–3544.

Wang, H. C., and John, W. (1988). Characteristics of Berner Impactor for Sampling Inorganic Ions, *Aerosol Sci. Technol.* 8:157–172.

Whitby, K. T., and Svendrup, G. M. (1980). California Aerosols: Their Physical and Chemical Characteristics, *Adv. Environ. Sci. Technol.* 10:477.

Zhang, X., and McMurry, P. H. (1987). Theoretical Analysis of Evaporative Losses from Impactor and Filter deposits, *Atmos. Environ.* 21:1779–1789.

Zhang, X., and McMurry, P. H. (1992). Evaporative Losses of Fine Particulate Nitrates During Sampling, *Atmos. Environ.* 26A(18):3305–3312.